Indian Journal of Chemical Technology
Vol. 29, May 2022, pp. 325-329

A new Ca(II) coordination polymer: Structural characterization and treatment activity on childhood asthma

Wenxiao Yuan, Luliang Cai, Yanjiao Tang, Binsha Fu & Ling Wang*

Department of Pediatrics, Hainan Provincial People's Hospital, Haikou 570 000, China

E-mail: lingwang202108@163.com

Received 2 October 2021; accepted 20 April 2022

In the present study, a 3D coordination polymer with the chemical composition of$[(CH_3)_2NH_2][Ca(tcpbH)(H_2O)]$ (1) has been solvothermally obtained from a rigid tetracarboxylic acid ligand tetrakis-(4-carboxyphenyl)benzene (H_4tcpb) and alkaline-earth ion Ca^{II}. Complex 1 has been well studied via Fourier-transform infrared spectroscopy, elemental analysis (EA), TG analysis and single-crystal X-ray diffraction analysis. Its application values on the childhood asthma were determined and the internal principle has been discussed simultaneously. Firstly, the ELISA is utilized to measure the content of inflammatory cytokines released into the Broncho alveolar lavage fluid (BALF) after compound treatment. In addition to this, the real time RT-PCR was conducted to measure the relative expression levels of NF-κB signaling pathway in the alveolar epithelial cells.

Keywords: BALF, Coordination polymer, Childhood asthma, RT-PCR

Bronchial asthma is a chronic inflammatory case of respiratory tract, which is involved by assorted kinds of cellular components and different cells, such as mast cells, T-lymphocytes, eosinophils, respiratory tract epithelial cells and neutrophils[1]. The nosogenesis of asthma is not yet fully understood, but various studies have shown that it is a disease related to many factors such as heredity, immunity, infection, and environment[2].

In recent years, coordination polymers (CPs) have drew much attention because of their specific structural and topological characteristics. At the same time, CPs has broad application prospects in the fields of gas separation, reserve, catalytic reaction and sensing because of its structural setting and diversified functions[3-8]. Based on previous reports, the structural characteristics and functionality of CPs are related to lots of aspects, such as reaction medium, pH environment, reaction temperature, coordination mode of metal center, coordination capacity of organic ligands, quantity of matching points provided by ligands[9-11]. Among the above influencing factors, effective and appropriate paired organic ligands play an important role in constructing innovative CPs. Thus, ligands based on tetracarboxylic acid have been favourably utilized in the formation of CPs[12-18]. On the basis of the above considerations, In the present study, a new 3D coordination polymer with the composition of$[(CH_3)_2NH_2][Ca(tcpbH)(H_2O)]$ (1) has been solvothermally obtained from a rigid tetracarboxylic acid ligand tetrakis-(4-carboxyphenyl)benzene (H_4tcpb) and alkaline-earth ion Ca^{II}. Complex 1has been well detected via Fourier-transform infrared spectroscopy, elemental analysis (EA), TG analysis and single-crystal X-ray diffraction analysis. The crystallographic analysis indicates that complex 1 exhibits a firm and 3-dimensional framework with a $\{4^4\cdot6^2\}^2\{4^8\cdot6^{16}\cdot8^4\}$ topology construction upon a 4,8-connected network. In the biological section, the treatment activation of the fresh compound against the childhood asthma was assessed, and the internal principle was discussed simultaneously.

Experimental Section

Chemicals and measurements

All reagents meet the quality standards for analysis, there is no need to further purification. Carbon, hydrogen and nitrogen were analyzed using the Perkin-Elmer 240C elemental analyzer. Fourier transform infrared (FT-IR) spectra were acquired via the Bruker Vector 22 FT-IR spectrophotometer with KBr pellets, ranging from 400 to 4000 cm^{-1}. Powder X-ray diffraction (PXRD) figures were recorded via the Shimadzu XRD-6000 X-ray diffractometer with Cu Kα (λ is 1.5418 Å) radiation at normal temperature. A Netzsch STA449 F1 thermal analyzer

was utilized to operate the TGA in an air environment with a heating speed of 10°C per minute, ranging from 25 to 800°C.

Preparation and characterization for $[(CH_3)_2NH_2][Ca(tcpbH)(H_2O)]$ (1)

A mixture of 2 mL H_2O and 0.5 mL formic acid, 5 mL DMF, 20 mg $tcpbH_4$ and 50 mg $Ca(ClO_4)_2·4H_2O$ was set in a 20 mL flask. Then it was kept at 393 K for 48 h. After lowering to the normal environment, achromatic bulk crystals were produced by filtration and washing. The yield was thirty-five percenton the basis of $tcpbH_4$. Anal. Cald. For $C_{36}H_{29}CaNO_9$: the carbon content is 65.54; the hydrogen content is 4.43; and the nitrogen content is 2.12 percent. Found: the carbon content is 65.23, the hydrogen content is4.25, the nitrogen content is 2.54. IR (KBr, cm^{-1}): 1588 (s), 1703(s), 1688(s), 3424 (s),1541 (m), 1392 (vs), 1119 (w),1467 (w), 786 (m),1178 (w), 745 (w), 1017 (m), 854 (w), 5542 (w), 722 (w).

To gather the data of X-ray, the Oxford X calibur E diffractometer was applied. Statistical analysis of diverse intensity data was recorded via CrysAlisPro software and the result was transferred into HKL format. The pattern of SHELXS applying direct method was used toform the fundamental structure, and the pattern of SHELXL-2014 applying least square method was modified. Various inhomogeneous parameters are employed to refine non H atoms. Then, the whole H atoms adopting AFIX program link with the C atom. Table 1 reveals the particular data of complex **1**.

Table 1 ─ Experiment details and crystallographic results on mixture **1**.

Empirical formula	$C_{36}H_{29}CaNO_9$
Formula weight	659.68
Temperature/K	288.15(10)
Crystal system	orthorhombic
Space group	Pbca
a/Å	20.2631(13)
b/Å	10.1457(3)
c/Å	32.129(2)
α/°	90
β/°	90
γ/°	90
Volume/$Å^3$	6605.3(6)
Z	8
$\rho_{calc}g/cm^3$	1.327
μ/mm^{-1}	0.246
Independent reflections	7571 [R_{int} = 0.0979, R_{sigma} = 0.0455]
Data/restraints/parameters	7571/0/439
Goodness-of-fit on F^2	1.053
Final R indexes [I>=2σ (I)]	R_1 = 0.0524, ωR_2 = 0.1217
Final R indexes [all data]	R_1 = 0.0805, ωR_2 = 0.1398
Largest diff. peak/hole / e $Å^{-3}$	0.63/-1.03
CCDC	2113437

ELISA determination

The ELISA assay was conducted in the study to measure the content of the inflammatory cytokines delivered into the alveolar lavage fluid. This conduction was carried out in accordance with the instructions. Briefly, fifty BALB/c rat utilized in the current study were obtained from the Nanjing University. All the rats were maintained in a standard experimental environment (20 to 25 g) for 3 days. LPS was used to influence the asthma model. Next, the compound was added at the content of 1, 2 and 5/kg. After treated with the compound, the alveolar lavage fluid was gathered from all the animal and the groups, and the number of the inflammatory cytokines delivered into the BALF was determined by indicated ELISA kit.

Real time RT-PCR detection

After the asthma model establishment and injection with the compound, the activation of NF-κB signaling pathway in the alveolar epithelial cells was determined via real time RT-PCR. All operations during the experimental followed the manufacturer's instructions with some appropriate modifications. In short, LPS was used to influence the asthma model. Next, the compound was added at the content of 1,2 and 5mg/kg. After treated with the compound, the alveolar epithelial cells were isolated and the whole RNA in the alveolar epithelial cells was separated from TRIZOL reagent. Finally, the relative expression levels of the *nf-κ b*and *p53* was assessed via real time RT-PCR, using the *gapdh* as the built-in control. The figures were counted by the $2^{-\Delta\Delta Ct}$ method from three preformation. The whole experimental procedure was manipulated 3 times, and the data was expressed as mean ±SD.

Results and Discussion

Structural characterization

The single crystal X-ray diffraction figures illustrate that 1 depicts a three-dimension framework locating in the space group *Pbca*. The asymmetric part of 1 composes of a single $[(CH_3)_2NH_2]^+$cation, a singlet cpbH ligand, a single water molecule and a single distinctive Ca^{2+} ion. Figure 1 (a) describes that the Ca^{2+} is octahedral coordination via five O atoms on different carboxylic groups, containing four $COO^-$and a single no-protonation COOH groups via a

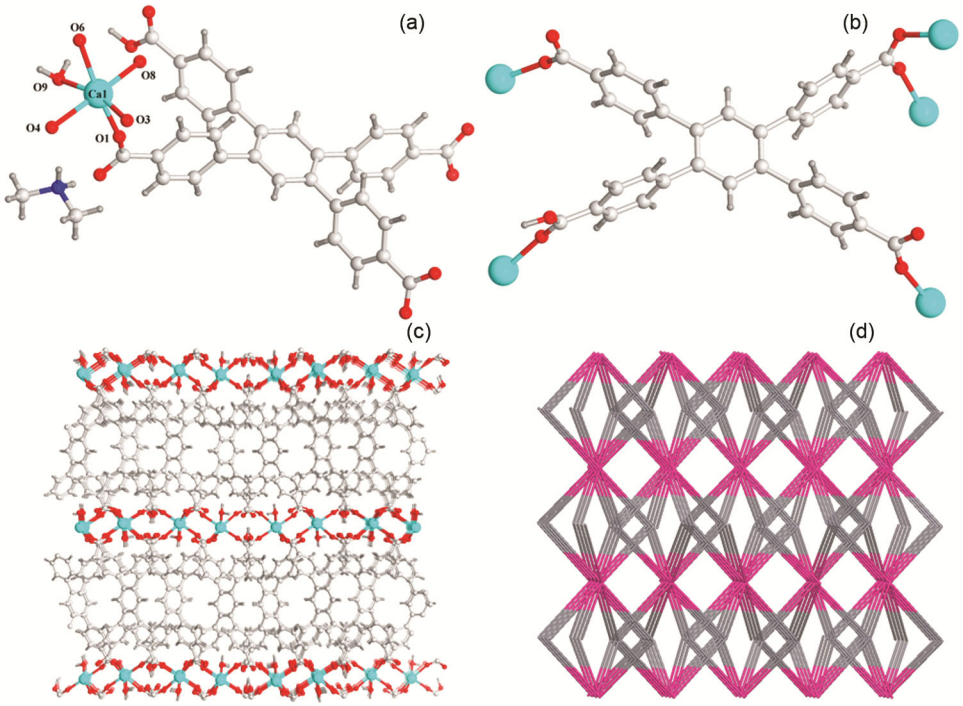

Fig. 1 — (a) Coordination surrounding for the Ca ion; (b) Coordination mode for the ligand; (c) Three-dimensional network of 1 and (d) 4,8-connection net of 1.

monodentate coordination pattern, and the final coordination place is held by the final water molecule. Double Ca^{2+}ions are linked through double carboxylic groups to construct a dimer of $[Ca_2(COO)_8(H_2O)_2]^{4-}$using as the SBU for 1. The distance of Ca–O is 2.3107(15) and 2.3510(15) Å. Every dimer SBU is linked via the tcpbH ligand with a single coordination pattern to construct a fresh three-dimensional framework with cage cavities along with the*a*-axis [Figs 1(b) and 1(c)]. The cage projected by a yellow ball composes of four tcpbH ligands connecting nine dimer SBUs. While, because of the fluence of the methyl group in the tcpbH ligand, access between neighboring cages is broken. From the aspect of topology, 1 construct a $\{4^4\cdot6^2\}^2\{4^8\cdot6^{16}\cdot8^4\}$ topology framework upon a 4,8-connected network [Fig. 1(d)]. Moreover, H-bonding forms between the carboxylic O atoms and H atoms in the final H_2O water molecule, and the dimethylamine ions form a powerful hydrogen-bonding net in 1.

To test the phase purity of the compound 1, PXRD experiments have been operated for the prepared samples [Fig. 2(a)]. The peak sites of the experiment and simulated PXRD figures are in accordance with others, showing that the crystal frame work is really representative of the blocky crystal compound. The discrepant in intensity could be on account of the preferential orientation of the crystals. In order to study the thermal stability of 1, we implemented a TGA check. TGA data of 1 is measured in the condition of nitrogen environment with a heating speed of 10°Cper minute in the temperature range of 25-600 °C. As shown in Fig. 2b, there are three stages of weight loss for 1, and the first weigh loss in of 3.2% the temperature range of 140-180°C should be attributed to the removal of one lattice molecule (calcd: 2.8%). The second weight loss of 7.2% from 250 to 400 °C should be related to the decomposition of one lattice $NHMe_2$ molecule (calcd: 6.8%), after which the third weight loss could be observed till the temperature of 600 °C, corresponding to the decomposition of the entire structure due to the loss of the organic ligand.

Compound significantly inhibiting the releasing of inflammatory cytokines into the alveolar lavage fluid

After the formation of the fresh compound, its biological activation was evaluated. During the procession of the asthma, there was commonly associated with an improved level of the inflammatory cytokines releasing into the alveolar lavage fluid. Therefore, the ELISA assay was firstly implemented to measure the content of inflammatory cytokines in the alveolar lavage fluid after compound treatment. Figure 3 explains that in the model group, there was an obvious improved level of inflammatory

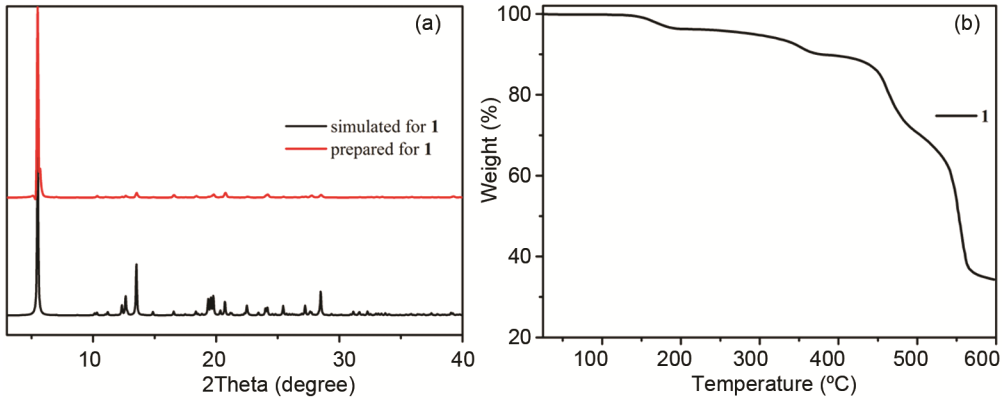

Fig 2. — (a) PXRD pictures for 1 and (b) TGA curve for 1.

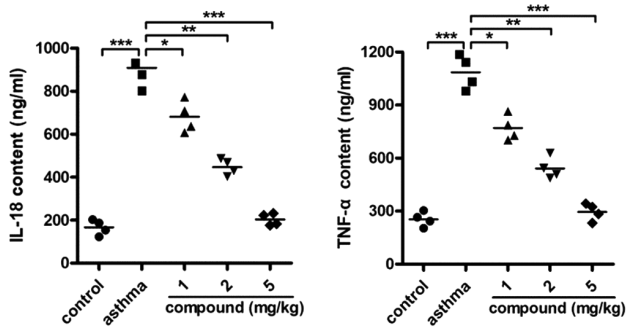

Fig. 3 — Obviously suppressed delivering of inflammatory cytokines into the BALF by the compound exposure. The asthma animal group was established and the new compound was added. ELISA assay was used to measure the number of inflammatory cytokines in the BALF.

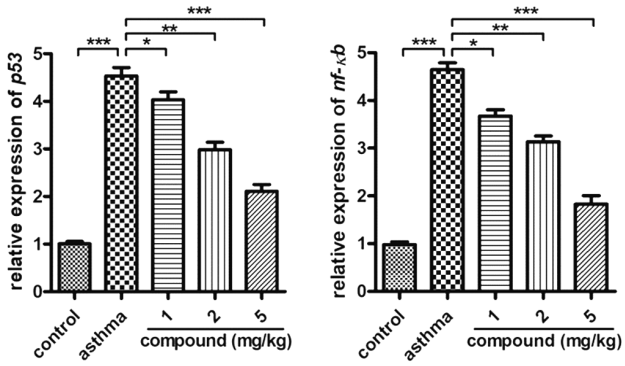

Fig. 4 — Dramatically reduced activity of NF-κB signaling pathway in the alveolar epithelial cells after injected with the compounds. Asthma animal group was constructed and the new compound was added for injection. The activation of NF-κB signaling pathway in the alveolar epithelial cells was measured via real time RT-PCR.

cytokines in the alveolar lavage fluid. After the treatment of the new compound, the delivering of inflammatory cytokines into the BALF was obviously inhibited. The inhibition of the new compound exhibited a dose relationship.

Compound obviously reduced the activation of NF-κB signaling pathway in the alveolar epithelial cells

In the above research, it has been proved that the compound played a significant role in reducing the content of inflammatory cytokines in the BALF. As the NF-κB signaling pathway regulates the expression and releasing of inflammatory cytokines. So, the activation of NF-κB signaling pathway in the alveolar epithelial cells after injecting the compounds was further determined via real time RT-PCR. In Figure 4, we got this information, the promotion of NF-κB signaling pathway in the experimental group was more effective than that of the control group, when P was less than 0.005. The activation of NF-κB signaling pathway may be reversed by the new compound in a dose-dependence method.

Conclusion

A fresh 3D coordination polymer has been created from a rigid tetracarboxylic acid ligand tetrakis-(4-carboxyphenyl)benzene (H_4tcpb) and alkaline-earth ion Ca^{II}. Complex 1 has been well detected by fourier-transform infrared spectroscopy, EA, TGA and single-crystal X-ray diffraction analysis. The crystallographic analysis indicates that complex 1 exhibits a firm and 3-dimensional framework with a $\{4^4\cdot6^2\}^2\{4^8\cdot6^{16}\cdot8^4\}$ topology construction upon a 4,8-connected network. The results of ELISA assay pointed out that the compound played a significant role in reducing the number of inflammatory cytokines delivered into the BALF. Besides, the compound could also significantly lower the expression levels of NF-κB signaling pathway dose dependently. Finally, it can be concluded that the compound has important application value on the childhood asthma by reducing the inflammatory response in the alveolar epithelial cells.

Reference

1 de Benedictis F M & Attanasi M, *Eur Respir Rev*, 25 (2016) 41.
2 Akar-Ghibril N & Phipatanakul W, *Curr Allergy Asthma Rep*, 20 (2020) 43.
3 Bazany-Rodríguez I J, Salomón-Flores M K, Viviano-Posadas A O, García-Eleno M A, Barroso-Flores J, Martínez-Otero D & Dorazco-González A, *Dalt Trans*, 50 (2021) 4255.
4 Wang M F, Mi Y, Hu F L, Niu Z, Yin X H, Huang Q, Wang H F & Lang J P, *J Am Chem Soc*, 142 (2020) 700.
5 Liu C Y, Chen X R, Chen H X, Niu Z, Hirao H, Braunstein P & Lang J P, *J Am Chem Soc*, 142 (2020) 6690.
6 Wang J, Chen N N, Zhang C, Jia L Y & Fan L, *Cryst Eng Comm*, 22 (2020) 811.
7 Hasanzadeh Esfahani M & Behzad M, *J Coord Chem*, 73 (2020) 154.
8 Wu K, Hu J, Shi S, Li J & Cheng X, *Dye Pigment*, 173 (2020) 107993.
9 Sen R, Halder A & Ghoshal D, *Polyhedron*, 183 (2020) 114534.
10 Bharati A K, Lama Somnath P & Siddiqui K A, *Inorganica Chim Acta*, 500 (2020) 119219.
11 Shi Y S, Hao Z C, Han C & Cui G H, *J Mol Struct*, 1201 (2020) 127218.
12 Kang W C, Han C, Liu D & Cui G H, *Inorg Chem Commun*, 106 (2019) 81.
13 Gao L, Zhang J, Zhai L, Liang J, Liang J, Niu X & Hu T, *Polyhedron*, 164 (2019) 90.
14 Gu J, Wen M, Cai Y, Shi Z, Arol A S, Kirillova M V & Kirillov A M, *Inorg Chem*, 58 (2019) 2403.
15 Du J L, Zhang X Y, Li C P, Gao J P, Hou J X, Jing X, Mu Y J & Li L J, *Sensors Actuators B Chem*, 257 (2018) 207.
16 Wang X L, Xiong Y, Liu X X, Liu G C, Lin H Y & Wang X, *Polyhedron*, 151 (2018) 264.
17 Burgos-Lopez Y, Del Plá J, Balsa L M, León I E, Echeverría G A, Piro O E, García-Tojal J, Pis-Diez R, González-Baró A C & Parajón-Costa B S, *Inorganica Chim Acta*, 487 (2019) 31.
18 Liang X, Jia Y, Zhan Z & Hu M, *Appl Organomet Chem*, 33 (2019) 15399.